Article

J. Biol. Regul. Homeost. Agents. 2024; 38(7): 5551–5561
https://doi.org/10.23812/j.biol.regul.homeost.agents.20243807.446

TMPRSS2 Affects SIRT1 Expression and NLRP3 Activity and Promotes the Progression of Pneumonia

Hongli Tian[1], Wenzhi Zhang[1], Yuehui Meng[1,*]

[1]Respiratory Medicine, The Fourth Hospital of Cangzhou City (Nanpi County People's Hospital), 061500 Cangzhou, Hebei, China
*Correspondence: myh3452024@163.com (Yuehui Meng)
Submitted: 29 March 2024 Revised: 9 May 2024 Accepted: 16 May 2024 Published: 1 July 2024

Background: Pneumonia is an inflammatory disease characterized by infection in the lung tissue. Transmembrane Protease Serine 2 (TMPRSS2) is implicated in the onset of inflammatory conditions. However, the precise role of TMPRSS2 in regulating the inflammatory response during pneumonia remains unclear. Hence, this research aims to explore the involvement of TMPRSS2 in pediatric pneumonia and unravel the associated mechanisms.

Methods: To induce pneumonia, lipopolysaccharide (LPS) was injected into the lungs of mice, establishing a mouse model of pneumonia. RAW264.7 cells served as an *in vitro* model for macrophages and underwent a 4-hour LPS stimulation. The expression pattern of TMPRSS2 in the pneumonia model was determined through quantitative reverse transcription polymerase chain reaction (qRT-PCR) and western blotting. TMPRSS2's impacts on the inflammatory response, lung tissue damage, oxidative stress levels, mitochondrial permeability, and nucleotide-binding oligomerization domain-like receptor protein 3 (NLRP3) expression in pneumonia were assessed through Enzyme-Linked Immunosorbent Assay (ELISA), hematoxylin and eosin (HE) staining, qRT-PCR, and cellular immunofluorescence experiments. The effects of TMPRSS2 knockdown and overexpression on the expression of NLRP3 and Sirtuin 1 (SIRT1) were also investigated using western blotting.

Results: The expression of TMPRSS2 mRNA and protein was significantly upregulated in mouse lung tissues upon LPS treatment. TMPRSS2 was found to enhance inflammation and lung damage in mice with pneumonia. Conversely, suppressing TMPRSS2 expression alleviated inflammation and lung damage in mice with pneumonia. Additionally, overexpressing TMPRSS2 intensified the inflammatory response in LPS-stimulated RAW264.7 cells, whereas silencing TMPRSS2 attenuated inflammation. We further demonstrated that TMPRSS2 influences the development of pneumonia by inhibiting SIRT1 expression and inducing NLRP3 activity.

Conclusions: Our study suggests that TMPRSS2 promotes the inflammatory progression of pneumonia, and modulates the expression of NLRP3 inflammasome and SIRT1.

Keywords: TMPRSS2; pneumonia; NLRP3; SIRT1

Introduction

Respiratory infections, particularly pneumonia, continue to present challenges to global public health [1,2]. A comprehensive understanding of the intricate molecular mechanisms governing the progression of inflammatory responses in the lungs is imperative for the development of targeted therapeutic interventions [3,4]. In recent years, Transmembrane Protease Serine 2 (TMPRSS2), a serine protease, has emerged as a pivotal player in diverse physiological processes, ranging from viral infections to the regulation of inflammation [5,6]. This article aims to delve into the nuanced interplay between TMPRSS2, the nucleotide-binding oligomerization domain-like receptor protein 3 (NLRP3) inflammasome, and Sirtuin 1 (SIRT1), shedding light on their collective impact on the advancement of pulmonary inflammation.

TMPRSS2, initially recognized for facilitating viral entry, exhibits expression across various tissues, with a notable presence in the respiratory epithelium [7]. Its overexpression has been correlated with heightened severity in respiratory infections, prompting investigations into its broader functionalities beyond viral interactions [8]. While the NLRP3 inflammasome, a multiprotein complex, has been implicated in instigating inflammatory responses in diverse pathological conditions [9], including respiratory diseases, the regulatory mechanisms linking TMPRSS2 to NLRP3 activation and subsequent inflammation remain largely unexplored [10].

SIRT1, a class III histone deacetylase, has garnered considerable interest due to its anti-inflammatory properties and its capacity to modulate various cellular processes [11,12]. Recent findings suggested a potential crosstalk between TMPRSS2 and SIRT1, raising intriguing questions about their coordinated influence on the inflammatory milieu within the lungs [13]. Unraveling the connections between TMPRSS2, NLRP3, and SIRT1 holds promise

Journal of
BIOLOGICAL REGULATORS
and Homeostatic Agents

for providing novel insights into the complex network of molecular events governing pulmonary inflammation.

This article aims to provide a comprehensive review of the existing literature on TMPRSS2, NLRP3, and SIRT1 in the context of pulmonary inflammation. By synthesizing the current knowledge, we aim to elucidate how TMPRSS2 may serve as a molecular regulator, modulating both the NLRP3 inflammasome and SIRT1, thereby influencing the progression of inflammatory processes in the lungs. The integration of these diverse components into a unified framework could potentially unveil new therapeutic targets for managing and mitigating the impact of respiratory infections, including pneumonia.

In this research, we explore the involvement of TMPRSS2 in pneumonia and its underlying mechanisms. Furthermore, we examine current knowledge gaps and suggest prospective avenues for future studies, aiming to enhance our comprehension of the intricate molecular interactions governing the progression of pulmonary inflammation.

Materials and Methods

Mouse Model of Pneumonia

Eighteen male C57BL/6 mice, aged between 6 and 8 weeks old, weighing between 4 and 5 grams, were individually housed in a controlled environment. The environmental conditions were maintained at a temperature of 22 ± 3 °C, relative humidity of 50 ± 20%, and a 12-hour light-dark cycle. The C57BL/6 mice were obtained from Nanjing Junke Bioengineering Co., Ltd. (Nanjing, China). Mice were anesthetized with an intraperitoneal injection of pentobarbital sodium (50 mg/kg body weight). Following anesthesia, mice in the pneumonia group received an intrapulmonary injection of lipopolysaccharide (LPS) (L8880, Solarbio, Beijing, China) at a dosage of 2 mg/kg body weight to induce pulmonary inflammation. Conversely, the sham-operated group received an equivalent volume of phosphate-buffered saline (PBS) (n = 6 per group) (P1010, Solarbio, Beijing, China). The typical pathological changes in mouse lung tissue, along with an increase in inflammatory mediators in lung tissue or serum, can assess the success of the LPS-induced mouse pneumonia model. The LPS-induced mouse pneumonia model has a 100% success rate. After three days, the mice were euthanized, and tissue samples were collected. To evaluate the impact of TMPRSS2, recombinant TMPRSS2 protein (1 mg/kg) (P06391, Solarbio, Beijing, China) was co-administered with LPS into the lung tissue. Additionally, to further investigate TMPRSS2's role in the mouse model, a TMPRSS2 inhibitor (Camostat) (IC2310, Solarbio, Beijing, China) was injected at 5 mg/kg after LPS administration (1 mg/kg). After one week of treatment, the mice were euthanized via intraperitoneal injection of pentobarbital sodium at a dosage of 110 mg/kg. This study was approved by the ethics committee of The Fourth Hospital of Cangzhou City (Nanpi County People's Hospital), under approval number NY-LL-2017-002.

HE Staining

Lung tissue samples were immersed in a 4% paraformaldehyde solution for fixation during 24 h. Subsequently, the tissues underwent dehydration by gradually immersing them in ascending concentrations of ethanol, ultimately reaching 100% ethanol. If there is fat in the samples, a defatting process is performed. Following this, the tissues were immersed in molten paraffin wax and then embedded to provide support during sectioning. After sectioning was complete, the sections underwent deparaffinization, followed by staining with hematoxylin and eosin (HE) dye (G1120, Solarbio, Beijing, China). After staining, the tissue sections underwent a gradual decrease in ethanol concentration to facilitate dehydration and clarification, culminating in slide mounting. Finally, the stained sections were observed under a microscope (BH3-MJL, Olympus, Tokyo, Japan).

Cell Culture and Transfection

Plasmid Cytomegalovirus (pCMV)-*TMPRSS2* overexpression plasmid (sense: 5′-ATGAGTCTGCTCCTCTGCTGTCTTGGCCTCCAAAGAATCC-3′, antisense: 5′-GGATTCTTTGGAGGCCAAGACAGCAGAGGAGCAGACTCAT-3′), pCMV-negative control (NC) (sense: 5′-ATGGCCATCATCGAGCTGCATTAGCGCTCAGTCACCTTGC-3′, antisense: 5′-GCAAGGTGACTGAGCGCTAATGCAGCTCGATGATGGCCAT-3′), siRNA-*TMPRSS2* (sense: 5′-GGAUCUGAUUGAAGGCUAUTT-3′, antisense: 5′-AUAAGCCUUCAAUCAGAUCCG-3′), and siRNA-NC (sense: 5′-UUCUCCGAACGUGUCACGUTT-3′, antisense: 5′-ACGUGACACGUUCGGAGAATT-3′) were obtained from Sangon Biotech (Shanghai, China). RAW264.7 cells (iCell-m047, Saibaikang Biotech, Shanghai, China) were cultured in Dulbecco's Modified Eagle Medium (DMEM) supplemented (iCell-0001, Saibaikang Biotech, Shanghai, China) with 10% fetal bovine serum (FBS) (iCell-0500, Saibaikang Biotech, Shanghai, China), penicillin (100 U/mL), and streptomycin (100 mg/mL) (iCell-15140-122, Saibaikang Biotech, Shanghai, China). The cells were incubated at 37 °C and 5% CO_2. RAW264.7 cells were cultured until reaching 70–80% confluence to ensure optimal growth conditions. RAW264.7 cells were transfected using Lipofectamine 3000 (L3000001, Thermo Fisher Scientific, Wilmington, MA, USA). After 48 h of transfection, RAW264.7 cells were treated with 0.1 mg/mL LPS or PBS for 4 h. This study has utilized RAW264.7 cells, which have been identified for species (STR, short tandem repeat) and tested negative for mycoplasma contamination.

Quantitative Real-Time PCR

First, total RNA was extracted from the samples using the TRIzol Universal Total RNA Extraction kit (12183555, Thermo Fisher Scientific, Wilmington, MA, USA). Reverse transcription was then performed using reverse transcriptase to generate the corresponding cDNA (K1622, Thermo Fisher Scientific, Wilmington, MA, USA). Specific primer pairs, including forward and reverse primers, were designed for the target gene. When preparing the quantitative polymerase chain reaction (qPCR) reaction mixture, the following components were combined: the reverse transcription product (cDNA), primer pairs specific to the target genes, fluorescent dyes (FP205, TIANGEN, Beijing, China), as well as the appropriate buffer and enzymes. After setting the parameters on the qPCR instrument, the reaction mixture was loaded into a PCR plate or optical reaction tubes. The qPCR was then conducted, involving initial denaturation, amplification, and fluorescence detection stages. By interpreting the signal strength data recorded by the qPCR instrument (CFX96, Bio-Rad Laboratories, Hercules, CA, USA), the relative expression levels of the target genes in each sample were calculated. To validate the reliability of the experiment, the repeatability and statistical significance of the experimental results were thoroughly assessed. The $2^{-\Delta\Delta Ct}$ method was used to analyze the experimental data. The primer sequences utilized in this study are listed in Table 1.

Table 1. Sequences of primers used for qRT-PCR.

Primer name	Primer sequence (5′-3′)
TMPRSS2-F	GAGAACCGTTGTGTTCGTCTC
TMPRSS2-R	GCTCTGGTCTGGTATCCCTTG
TNF-α-F	GCCTCTTCTCATTCCTGCTTG
TNF-α-R	GGCCATTTGGGAACTTCTCA
IFN-γ-F	ATGAACGCTACACACTGCATCTTGG
IFN-γ-R	TGGCTCTGCAGGATTTTCATG
β-*Actin*-F	ACACTGTGCCCATCTACG
β-*Actin*-R	TGTCACGCACGATTTCC

qRT-PCR, quantitative reverse transcription polymerase chain reaction; *TMPRSS2*, Transmembrane Protease Serine 2; *TNF*-α, Tumor Necrosis Factor-alpha; *IFN*-γ, Interferon-gamma.

Western Blotting

Total proteins were extracted from myometrial tissue and RAW264.7 cells using a protein extraction reagent (78510, Thermo Fisher Scientific, Wilmington, MA, USA). The target proteins were separated through sodium dodecyl sulfate polyacrylamide gel electrophoresis (SDS-PAGE) electrophoresis and then transferred onto a poly(vinylidene fluoride) (PVDF) membrane. Subsequently, the membrane was immersed in a 5% blocking buffer for 1 h to prevent non-specific binding. Primary antibodies were then applied to the PVDF membranes and allowed to incubate. The antibodies used were: TMPRSS2 (1:1000 dilution; cat no. ab214462, Abcam, Cambridge, UK), NLRP3 (1:1000 dilution; cat no. ab263899, Abcam, Cambridge, UK), SIRT1 (1:1000 dilution; cat no. ab110314, Abcam, Cambridge, UK), and Glyceraldehyde-3-Phosphate Dehydrogenase (GAPDH) (1:1000 dilution; cat no. Ab8245, Abcam, Cambridge, UK). The membranes were then incubated with horseradish peroxidase (HRP)-labeled anti-rabbit secondary antibodies (1:2000 dilution; cat no. ZB-2305, ZB-2301, ZSGB-BIO, Beijing, China) for 1 h at room temperature. The chemiluminescent signal from the target band was detected using a chemiluminescence instrument (P0018S, Beyotime, Shanghai, China). Finally, the intensity of the gray value was quantified using ImageJ software (version 1.5f, National Institutes of Health, Bethesda, MD, USA).

ELISA Experiments

The concentrations of malondialdehyde (MDA) (A003-1-2), superoxide dismutase (SOD) (A001-3-2), glutathione (GSH) (A006-2-1), Reactive Oxygen Species (ROS) (E004-1-1), Interleukin (IL)-1β (H002-1-2), and IL-6 (H007-1-1) in the cell extracts were quantified using Enzyme-Linked Immunosorbent Assay (ELISA) kits from Nanjing Jiancheng Biological Engineering Institute (Nanjing, China), following the manufacturer's instructions. The optical density (OD) values at 450 nm were measured using a microplate reader (Cmax plus, Molecular Devices, Silicon Valley, CA, USA).

Cell Fluorescent Staining

RAW264.7 cells were fixed in a culture dish with 4% paraformaldehyde for 20 min. The cells were permeabilized using a 0.1% Triton X-100 solution to enhance cell membrane permeability. Non-specific binding sites were blocked by adding 5% Bovine Serum Albumin (BSA) to the cells. The cells were incubated with specific NLRP3 antibodies (1:1000 dilution; cat no. ab263899, Abcam, Cambridge, UK), Mitotracker Green fluorescent dye (M7514, Thermo Fisher Scientific, Wilmington, MA, USA), or 2′,7′-Dichlorofluorescin Diacetate (DCFDA) dye (C369, Thermo Fisher Scientific, Wilmington, MA, USA) at 4 °C overnight or at room temperature for 1 h. The cells were washed with PBS. Subsequently, a fluorescent-labeled secondary antibody such as Alexa Fluor (1:1000 dilution; cat no. ab150077, Abcam, Cambridge, UK) was added to the cells to visualize the NLRP3 protein. 4′,6-Diamidino-2-Phenylindole (DAPI) was employed for nuclear staining. The fluorescence signals were observed in the cell samples using a fluorescence microscope (FV3000, Olympus, Tokyo, Japan).

Journal of
BIOLOGICAL REGULATORS
and Homeostatic Agents

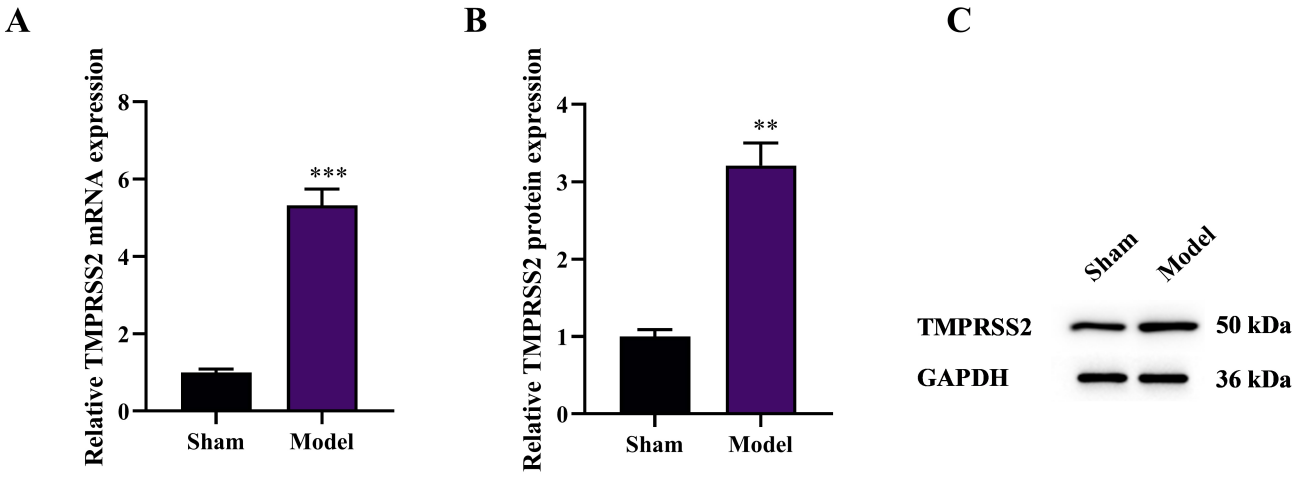

Fig. 1. TMPRSS2 expression is upregulated in pneumonia. (A) mRNA expression levels of *TMPRSS2* in lung tissues. (B,C) Protein expression levels of TMPRSS2 in lung tissues. (n = 6). $^{**}p < 0.01$, $^{***}p < 0.001$. GAPDH, Glyceraldehyde-3-Phosphate Dehydrogenase.

Statistical Analysis

The data analysis for this study was conducted using GraphPad Prism software (version 9.5, GraphPad Software, Inc., San Diego, CA, USA; https://www.graphpad-prism.cn/). The results were expressed as mean ± standard deviation (SD). For comparisons between two groups, a *t*-test was utilized, while one-way analysis of variance (ANOVA) was employed for multiple-group comparisons. Statistical significance was defined as $p < 0.05$.

Results

The Expression of TMPRSS2 is Upregulated in a Mouse Model of Pneumonia

The results from quantitative real-time polymerase chain reaction (qRT-PCR) and western blot analysis corroborated a significant upregulation in both mRNA and protein expression levels of TMPRSS2 in the lung tissues of the pneumonia mouse model, compared to the sham surgery group ($p < 0.01$ and $p < 0.001$, respectively) (Fig. 1A–C). These findings suggest a strong correlation between the elevated TMPRSS2 expression in the lung tissues of pneumonia mice and the presence of inflammation.

Enhanced Expression of TMPRSS2 Induces Inflammation and Intensifies Pulmonary Injury in Mice Afflicted with Pneumonia

To elucidate the role of TMPRSS2 in pneumonia, we administered recombinant TMPRSS2 protein along with LPS into the pulmonary tissues of mice. This resulted in an elevation of hemoglobin (Hgb) and enhanced neutrophil infiltration in the bronchoalveolar lavage (BAL) fluid ($p < 0.05$ and $p < 0.001$, respectively) (Fig. 2A,B). Hematoxylin and eosin (HE) staining revealed that TMPRSS2 exacerbated lung tissue damage (Fig. 2E). Additionally, TMPRSS2 protein elevated the levels of inflammatory cytokines, such as Tumor Necrosis Factor-alpha (TNF-α), Interferon-gamma (IFN-γ), IL-1β, and IL-6, in lung tissue (Fig. 2C,D,F,G). TMPRSS2 protein also induced oxidative stress, as evidenced by an increase in the levels of MDA in lung tissue and a decrease in the levels of SOD and GSH ($p < 0.001$) (Fig. 2H–J).

Silencing TMPRSS2 Suppresses Inflammation and Lung Damage in Mice with Pneumonia

Subsequently, we utilized the TMPRSS2 inhibitor (camostat mesylate) to explore whether suppressing TMPRSS2 activity could protect against lung damage in mice with pneumonia. The TMPRSS2 inhibitor significantly reduced the concentrations of Hgb and neutrophil infiltration in BAL fluid ($p < 0.05$ and $p < 0.001$, respectively) (Fig. 3A,B). HE staining revealed that the TMPRSS2 inhibitor alleviated lung tissue damage (Fig. 3E). Additionally, the TMPRSS2 inhibitor markedly decreased the levels of inflammatory cytokines, such as TNF-α, IFN-γ, IL-1β, and IL-6, in lung tissue ($p < 0.05$ and $p < 0.01$) (Fig. 3C,D,F,G). Moreover, the TMPRSS2 inhibitor mitigated oxidative stress, evidenced by a decrease in MDA levels within lung tissue and an increase in SOD and GSH levels ($p < 0.001$) (Fig. 3H–J). These findings suggest that TMPRSS2 plays a pivotal role in inflammation and lung damage in pediatric pneumonia.

Overexpression of TMPRSS2 Promotes the Inflammatory Response in RAW264.7 Macrophage Cells

Macrophages play a crucial role in pulmonary inflammation. To investigate the function of TMPRSS2 in these immune cells, we transfected RAW264.7 cells with a TMPRSS2 overexpression plasmid or TMPRSS2 siRNA, fol-

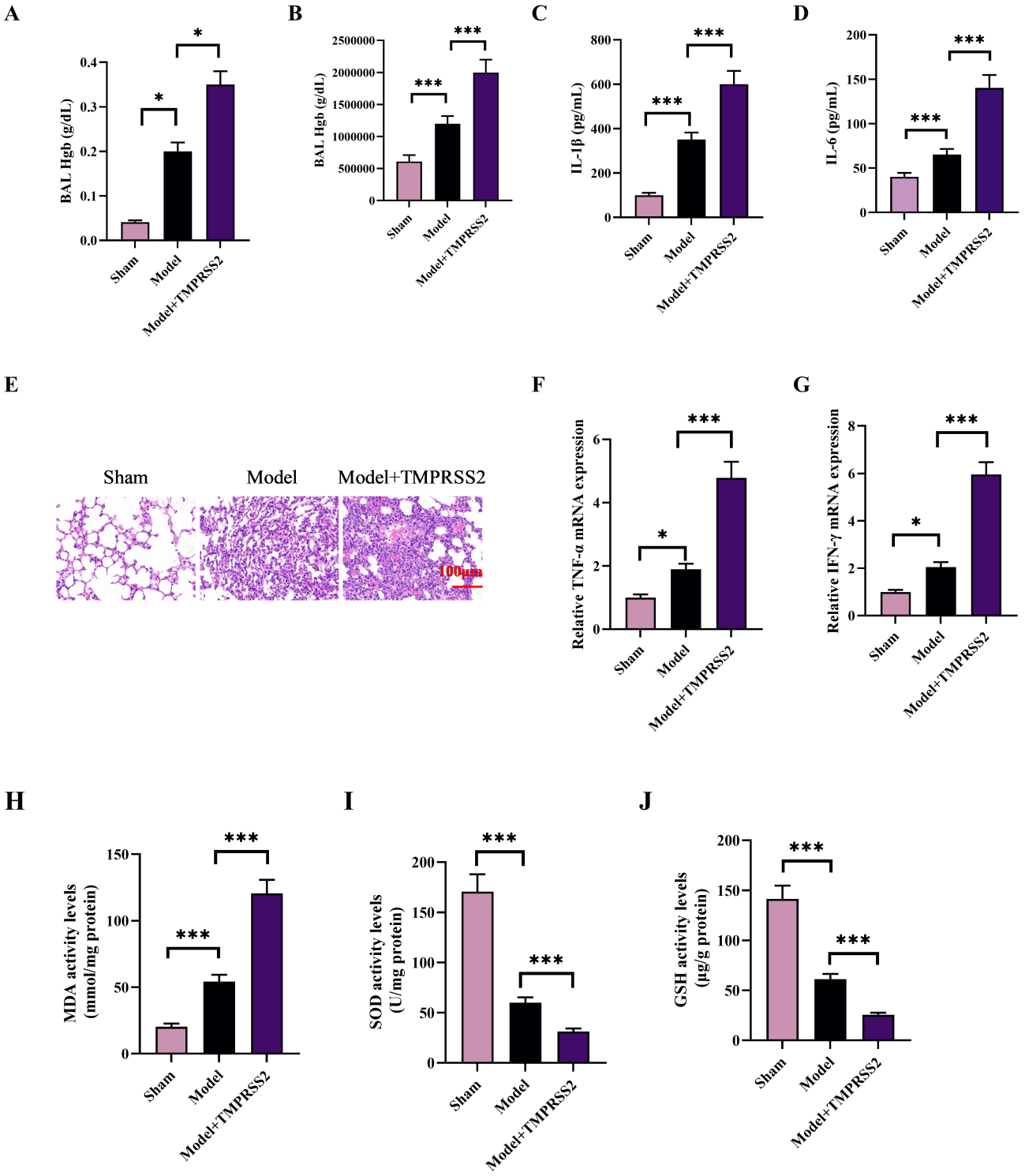

Fig. 2. The TMPRSS2 protein induces inflammation and pulmonary damage in mice with pneumonia. (A) Concentrations of hemoglobin (Hgb) in BAL fluid. (B) Neutrophil levels in BAL fluid. (C,D) Levels of Interleukin (IL)-1β and IL-6 in lung tissue. (E) Hematoxylin and eosin (HE) staining of lung tissue. (F,G) mRNA levels of *TNF*-α and *IFN*-γ in lung tissue. (H–J) Concentrations of MDA, SOD, and GSH in lung tissue (n = 6). *$p < 0.05$ and ***$p < 0.001$. BAL, bronchoalveolar lavage; MDA, malondialdehyde; SOD, superoxide dismutase; GSH, glutathione.

lowed by LPS stimulation. As expected, the TMPRSS2 overexpression plasmid significantly increased the expression levels of TMPRSS2 ($p < 0.001$) (Fig. 4A). TMPRSS2 overexpression elevated the levels of IL-1β and IL-6, as well as the mRNA expression of *TNF*-α and *IFN*-γ ($p < 0.001$) (Fig. 4B–E). Conversely, si-*TMPRSS2* reduced

Journal of
BIOLOGICAL REGULATORS
and Homeostatic Agents

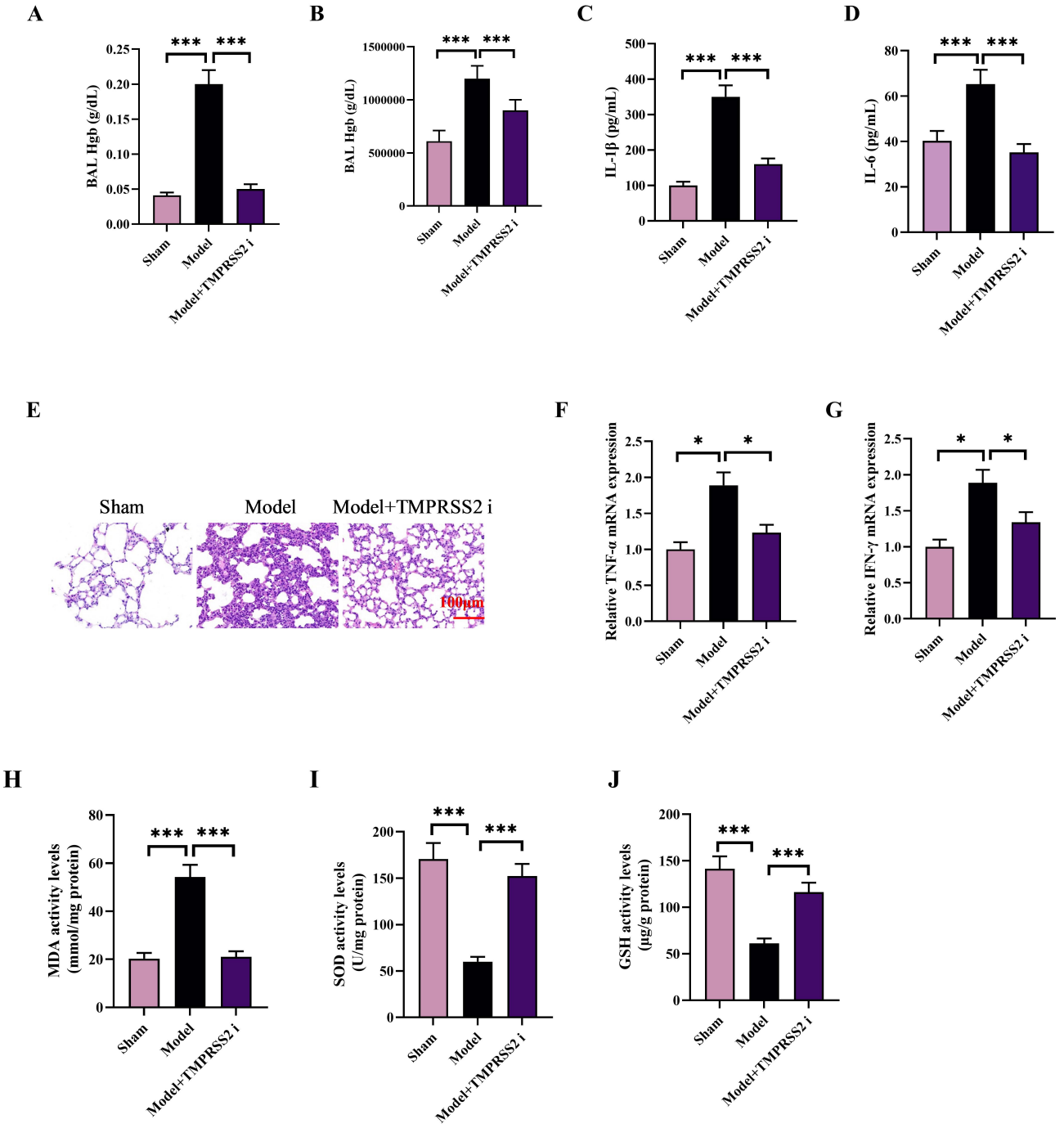

Fig. 3. Inhibiting TMPRSS2 can suppress inflammation and lung damage in mice. (A) Levels of Hgb in BAL fluid. (B) Levels of neutrophils in BAL fluid. (C,D) Levels of IL-1β and IL-6 in lung tissue. (E) HE staining of lung tissue. (F,G) mRNA levels of *TNF*-α and *IFN*-γ in lung tissue. (H–J) Levels of MDA, SOD, and GSH in lung tissue (n = 6). *$p < 0.05$ and ***$p < 0.001$.

the expression levels of TMPRSS2 ($p < 0.001$) (Fig. 4F). si-*TMPRSS2* also decreased the levels of IL-1β and IL-6, along with the mRNA expression of *TNF*-α and *IFN*-γ ($p < 0.001$) (Fig. 4G–J). Collectively, these data suggest that TMPRSS2 promotes an inflammatory response in macrophages.

TMPRSS2 Amplifies NLRP3 Expression while Inhibiting SIRT1 Expression

To investigate the inflammatory mechanisms mediated by TMPRSS2, we analyzed the protein expression of NLRP3 and SIRT1 in the lung tissues of three groups: a pneumonia mouse model group, a TMPRSS2 recombinant protein-treated group, and a TMPRSS2 inhibitor-treated group. Recombinant TMPRSS2 inhibited the protein lev-

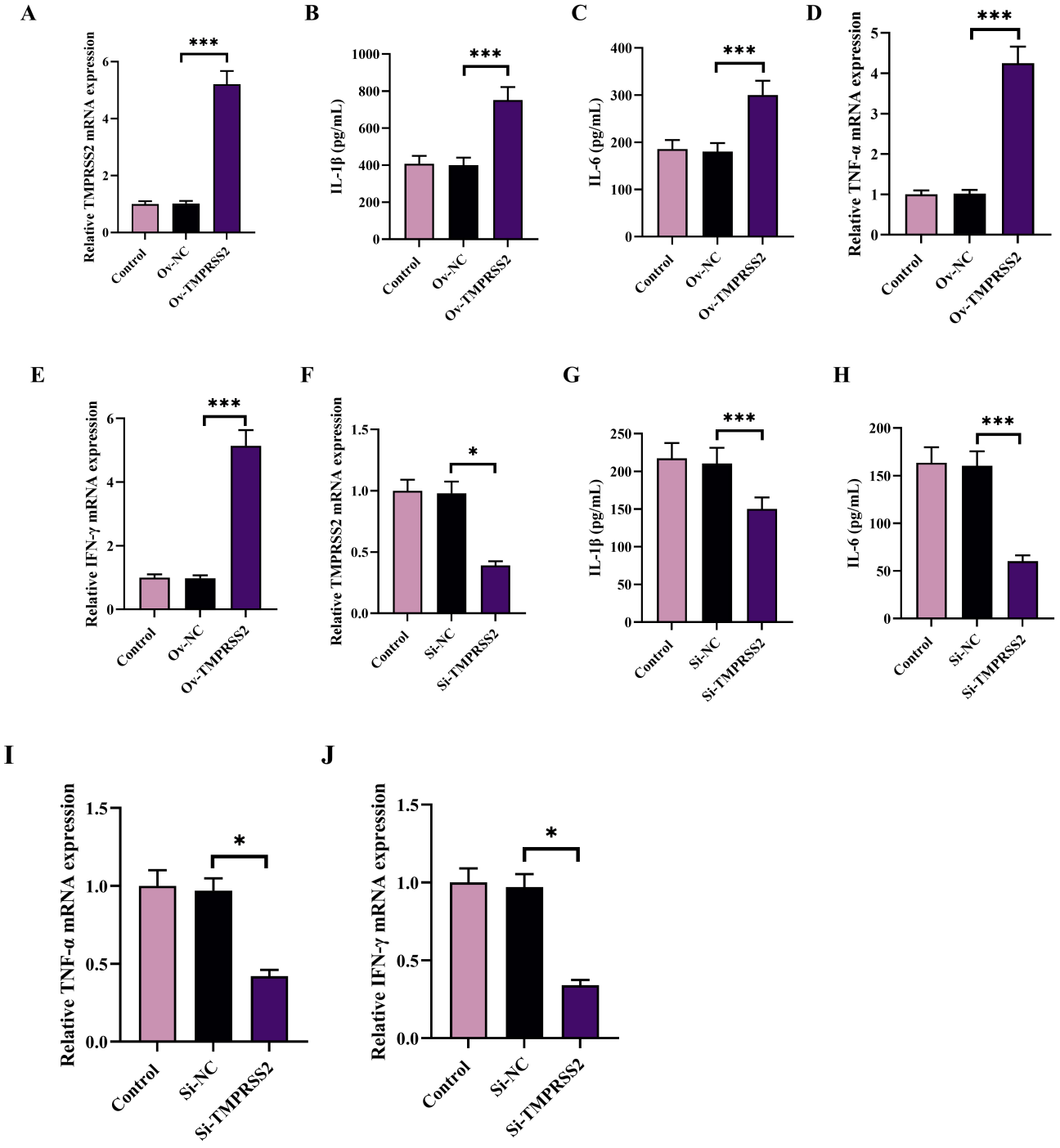

Fig. 4. TMPRSS2 modulates inflammation in a macrophage model *in vitro*. (A–E) Levels of TMPRSS2 (A), IL-1β (B), IL-6 (C), TNF-α (D), and IFN-γ (E) in RAW264.7 cells after TMPRSS2 overexpression. (F–J) Levels of TMPRSS2 (F), IL-1β (G), IL-6 (H), TNF-α (I), and IFN-γ (J) in RAW264.7 cells after TMPRSS2 knockdown (n = 6). *$p < 0.05$ and ***$p < 0.001$. NC, negative control.

els of SIRT1 while significantly elevating the protein levels of NLRP3 in the lung tissues of mice with pneumonia ($p < 0.001$) (Fig. 5A–C). Conversely, treatment with the TMPRSS2 inhibitor increased SIRT1 levels and inhibited NLRP3 levels in the lung tissues of pneumonia mice ($p < 0.001$) (Fig. 5D–F). These data suggest that TMPRSS2 promotes the expression of NLRP3 while concurrently inhibiting the expression of SIRT1.

TMPRSS2 Induces Inflammation by Activating the NLRP3 Inflammasome and Modulating Mitochondrial Permeability Transition

TMPRSS2 overexpression elevated TMPRSS2 and NLRP3 protein levels, while suppressing SIRT1 protein expression in RAW264.7 cells ($p < 0.05$ and $p < 0.01$) (Fig. 6A–D). This overexpression induced

Journal of
BIOLOGICAL REGULATORS
and Homeostatic Agents

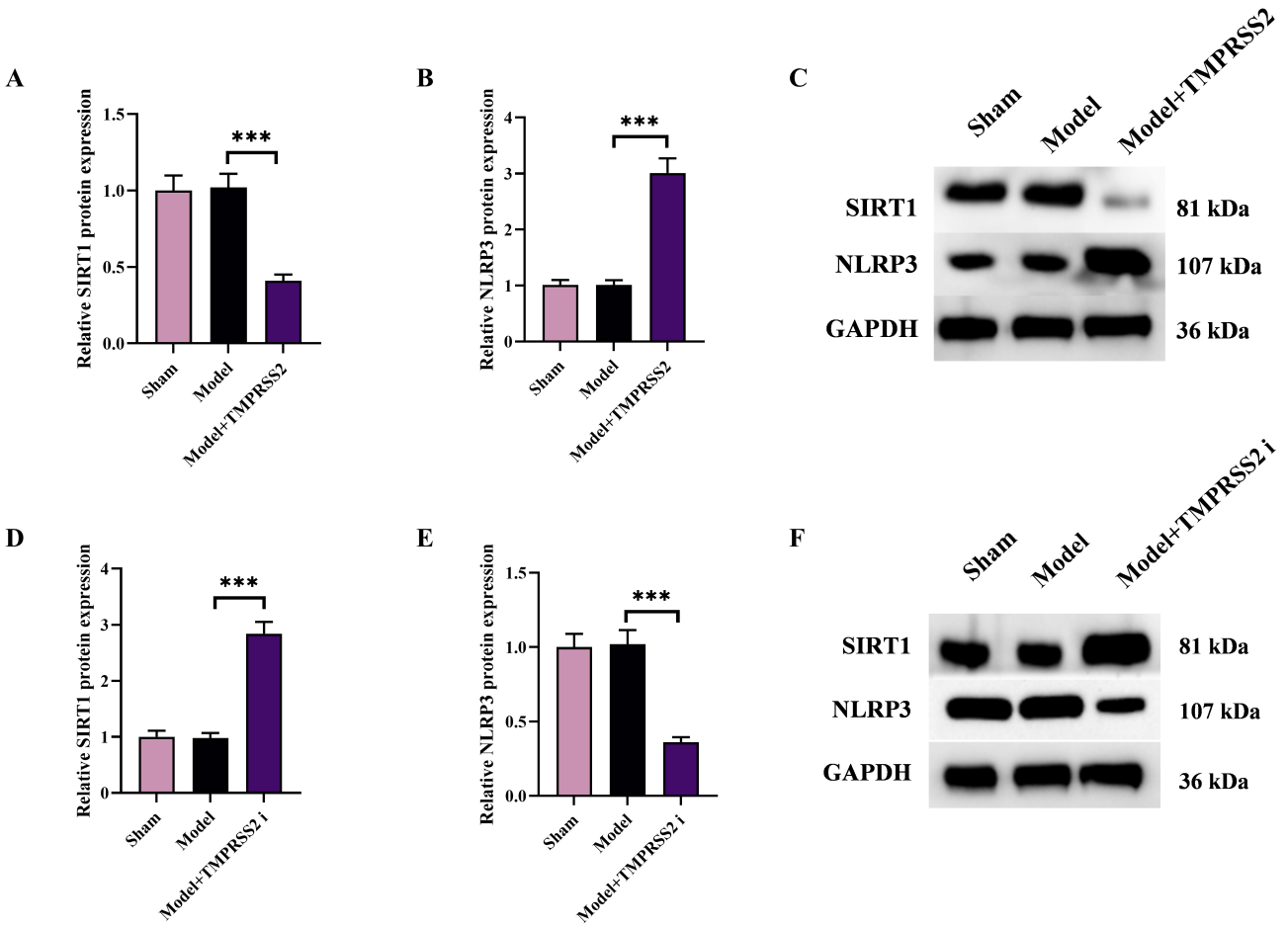

Fig. 5. TMPRSS2 promotes the expression of NLRP3 while inhibiting the expression of SIRT1. (A–C) Expression levels of NLRP3 and SIRT1 proteins in mice with pneumonia treated with recombinant TMPRSS2 protein. (D–F) Protein levels of NLRP3 and SIRT1 in mice with pneumonia treated with TMPRSS2 inhibitor. (n = 6). ***$p < 0.001$. SIRT1, Sirtuin 1; NLRP3, nucleotide-binding oligomerization domain-like receptor protein 3.

mitochondrial damage and stimulated NLRP3 protein expression in the macrophage model (Fig. 6E&E-1&E-2). Additionally, TMPRSS2 overexpression heightened ROS and MDA production, reduced SOD levels, and amplified 5,5′,6,6′-Tetrachloro-1,1′,3,3′-tetraethylbenzimidazolylcarbocyanine iodide (JC-1) staining in the macrophage model ($p < 0.05$ and $p < 0.001$, respectively) (Fig. 6F–I). Conversely, TMPRSS2 silencing decreased TMPRSS2 and NLRP3 expression while enhancing SIRT1 expression ($p < 0.05$ and $p < 0.01$) (Fig. 6J–M). It mitigated mitochondrial damage and suppressed NLRP3 expression in LPS-stimulated macrophages (Fig. 6N). TMPRSS2 knockdown also diminished ROS production and MDA levels, elevated SOD levels, and intensified JC-1 staining in the macrophage model ($p < 0.05$ and $p < 0.001$) (Fig. 6O–R). These findings suggest that TMPRSS2 induces inflammation in macrophages through NLRP3 inflammasome activation and compromises mitochondrial function by downregulating SIRT1.

Discussion

Patients with pneumonia not only suffer from severe pulmonary conditions but also experience multi-organ damage throughout the body [14,15]. In this investigation, we demonstrated an elevation of TMPRSS2 levels in mice afflicted with pneumonia. Research by Yao and Lawrence [16] suggested a close association between TMPRSS2 and mitochondrial function, linking it to mitochondrial homeostasis and autophagic clearance. Our findings indicate that the increased expression of TMPRSS2 in pneumonia could potentially exacerbate inflammatory responses and oxidative stress.

Oxidative stress is prevalent throughout the body and plays essential roles in various physiological functions [17]. When confronted with pathogenic infections and other adverse stimuli, an excess of free radicals can lead to oxidative damage in different intracellular molecules and components [18]. Research indicates that after the onset of pneumonia, the release of hydrogen peroxide and superoxide radicals in the lungs can be regulated [19]. Oxidative stress-

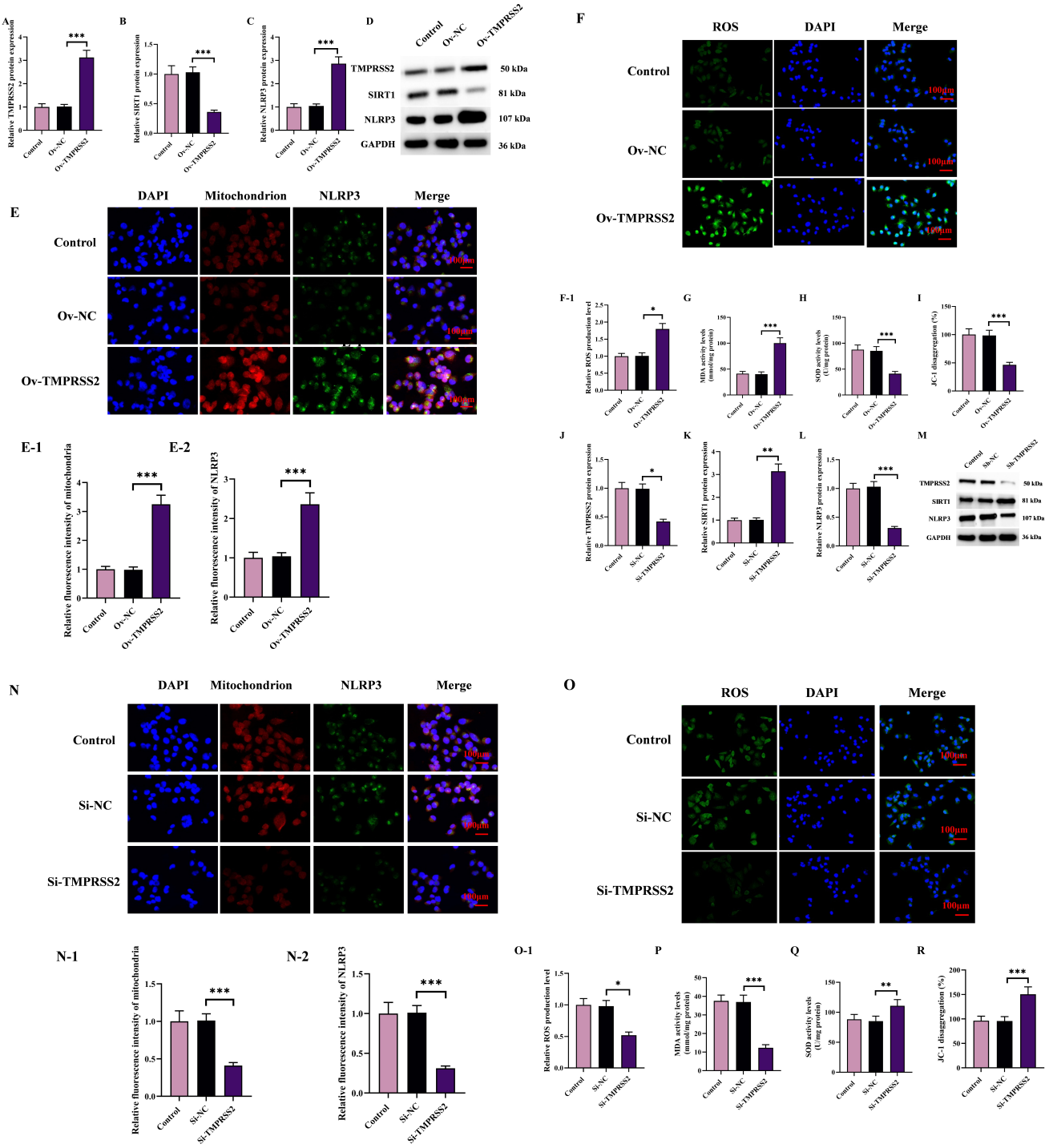

Fig. 6. TMPRSS2 promotes inflammation in pneumonia by upregulating NLRP3 inflammasome and downregulating SIRT1. (A–D) Protein expression of TMPRSS2, SIRT1, and NLRP3 in RAW264.7 macrophages overexpressing TMPRSS2. (E) Mitochondrial permeability transition and NLRP3 expression in macrophages overexpressing TMPRSS2. (E-1,E-2) Quantitative analysis of relative fluorescence intensity of mitochondria (E-1) and NLRP3 (E-2). (F,F-1) Levels of ROS production. (G) MDA levels. (H) SOD levels. (I) JC-1 depolarization levels. (J–M) Protein expression of TMPRSS2, SIRT1, and NLRP3 in RAW264.7 macrophages overexpressing TMPRSS2. (N,N-1,N-2) Mitochondrial permeability transition and NLRP3 expression in macrophages overexpressing TMPRSS2. (O,O-1) Levels of ROS production. (P) MDA levels. (Q) SOD levels. (R) JC-1 depolarization levels. (*$p < 0.05$, **$p < 0.01$, and ***$p < 0.001$). ROS, Reactive Oxygen Species; JC-1, 5,5′,6,6′-Tetrachloro-1,1′,3,3′-tetraethylbenzimidazolylcarbocyanine iodide.

Journal of
BIOLOGICAL REGULATORS
and Homeostatic Agents

induced lung injury is linked to the onset and progression of pneumonia [20]. Our findings indicate that the recombinant TMPRSS2 protein enhances inflammation and oxidative stress in the pneumonia model, and inhibiting its activity mitigates these detrimental responses. Study suggests that TMPRSS2 induces inflammatory responses, contributing to the development of inflammatory bowel disease [21]. All the aforementioned data collectively indicate that the TMPRSS2 protein plays a pivotal role in the inflammation associated with pneumonia.

Inflammation serves as a crucial factor contributing to vascular dysfunction, apoptosis of endothelial cells, and the aging process. A previous study indicated that during aging, vascular regeneration is impaired, and the expression levels of SIRT1 in endothelial cells decrease [22]. Endothelial cell aging is a crucial hallmark of vascular aging and a major contributor to cardiovascular diseases such as hypertension and atherosclerosis [23]. In our investigation, we observed that TMPRSS2 downregulates the expression of SIRT1 in the pneumonia model. Research has indicated that TMPRSS2 and SIRT1 are essential in the biological functions of the vascular endothelium during pediatric critical illnesses [13]. Our findings suggest that TMPRSS2 regulates inflammation and oxidative reactions in pneumonia by modulating the expression of SIRT1. However, the underlying biological mechanisms of SIRT1 expression remain worthy of further investigation to elucidate the intricate pathways.

The NLRP3 inflammasome identifies distinct molecular patterns, triggering the inflammatory response and resulting in the release of various inflammatory factors, including IL-18 and IL-1β [24]. Study suggests that the initial immune response to pulmonary stimuli is predominantly mediated by inflammasomes [25]. However, excessive inflammation can exacerbate tissue damage and contribute to the development of respiratory system diseases [26]. The onset and progression of respiratory diseases, such as infectious pneumonia, asthma, chronic obstructive pulmonary disease, and acute lung injury, are linked to inflammatory processes [27]. Excessive pro-inflammatory cytokines are detrimental to maintaining the homeostasis of inflammatory tissues. Our study results further suggest that TMPRSS2 inhibits the expression of NLRP3 in a pneumonia model.

Nevertheless, our research did not explore the mechanisms through which TMPRSS2 regulates NLRP3 expression in the pneumonia model. Subsequent investigations are warranted to elucidate how TMPRSS2 influences the expression of NLRP3 and SIRT1 in the pneumonia mouse model. Additionally, the potential signaling axis of SIRT1/NLRP3 may be crucial for the functionality of TMPRSS2 in pneumonia.

Conclusions

In summary, our investigation reveals that TMPRSS2 promotes inflammation and oxidative stress within a pneumonia model. Our findings suggest that TMPRSS2 suppresses SIRT1 expression, thereby intensifying mitochondrial permeability, and elevates NLRP3 levels, contributing to the regulation of inflammation in the pneumonia model.

Availability of Data and Materials

Data to support the findings of this study are available on reasonable request from the corresponding author.

Author Contributions

HT designed the research study; YM performed the research; WZ collected and analyzed the data. All authors have been involved in drafting the manuscript and all authors have been involved in revising it critically for important intellectual content. All authors gave final approval of the version to be published. All authors have participated sufficiently in the work to take public responsibility for appropriate portions of the content and agreed to be accountable for all aspects of the work in ensuring that questions related to its accuracy or integrity.

Ethics Approval and Consent to Participate

This study has been approved by the ethics committee of The Fourth Hospital of Cangzhou City (Nanpi County People's Hospital), under approval number NY-LL-2017-002.

Acknowledgment

Not applicable.

Funding

This research received no external funding.

Conflict of Interest

The authors declare no conflict of interest.

References

[1] Martin-Loeches I, Torres A, Nagavci B, Aliberti S, Antonelli M, Bassetti M, *et al*. ERS/ESICM/ESCMID/ALAT guidelines for the management of severe community-acquired pneumonia. Intensive Care Medicine. 2023; 49: 615–632.

[2] Seeger A, Rohde G. Community-acquired pneumonia. Deutsche Medizinische Wochenschrift (1946). 2023; 148: 335–341.

[3] Gan T, Yu J, He J. miRNA, lncRNA and circRNA: targeted molecules with therapeutic promises in Mycoplasma pneumoniae infection. Archives of Microbiology. 2023; 205: 293.

[4] Suberi A, Grun MK, Mao T, Israelow B, Reschke M, Grundler J, *et al*. Polymer nanoparticles deliver mRNA to the lung for

mucosal vaccination. Science Translational Medicine. 2023; 15: eabq0603.

[5] Lin L, Zeng F, Mai L, Gao M, Fang Z, Wu B, *et al*. Expression of ACE2, TMPRSS2, and SARS-CoV-2 nucleocapsid protein in gastrointestinal tissues from COVID-19 patients and association with gastrointestinal symptoms. The American Journal of the Medical Sciences. 2023; 366: 430–437.

[6] Pairo-Castineira E, Rawlik K, Bretherick AD, Qi T, Wu Y, Nassiri I, *et al*. GWAS and meta-analysis identifies 49 genetic variants underlying critical COVID-19. Nature. 2023; 617: 764–768.

[7] Tyagi K, Rai P, Gautam A, Kaur H, Kapoor S, Suttee A, *et al*. Neurological manifestations of SARS-CoV-2: complexity, mechanism and associated disorders. European Journal of Medical Research. 2023; 28: 307.

[8] Saunders N, Fernandez I, Planchais C, Michel V, Rajah MM, Baquero Salazar E, *et al*. TMPRSS2 is a functional receptor for human coronavirus HKU1. Nature. 2023; 624: 207–214.

[9] Gallenga CE, Maritati M, Mura M, Di Virgilio F, Conti P, Contini C. Macrophage Activation in Follicular Conjunctivitis during the COVID-19 Pandemic. Microorganisms. 2023; 11: 2198.

[10] Wilson GN. A Clinical Qualification Protocol Highlights Overlapping Genomic Influences and Neuro-Autonomic Mechanisms in Ehlers-Danlos and Long COVID-19 Syndromes. Current Issues in Molecular Biology. 2023; 45: 6003–6023.

[11] Jin Q, Liu T, Qiao Y, Liu D, Yang L, Mao H, *et al*. Oxidative stress and inflammation in diabetic nephropathy: role of polyphenols. Frontiers in Immunology. 2023; 14: 1185317.

[12] Liu MH, Lin XL, Xiao LL. Hydrogen sulfide attenuates TMAO induced macrophage inflammation through increased SIRT1 sulfhydration. Molecular Medicine Reports. 2023; 28: 129.

[13] Richter RP, Payne GA, Ambalavanan N, Gaggar A, Richter JR. The endothelial glycocalyx in critical illness: A pediatric perspective. Matrix Biology Plus. 2022; 14: 100106.

[14] Vieira PC, de Oliveira RB, da Silva Mendonça TM. Should oral chlorhexidine remain in ventilator-associated pneumonia prevention bundles? Medicina Intensiva. 2022; 46: 259–268.

[15] Mohsin M, Tabassum G, Ahmad S, Ali S, Ali Syed M. The role of mitophagy in pulmonary sepsis. Mitochondrion. 2021; 59: 63–75.

[16] Yao Y, Lawrence DA. Susceptibility to COVID-19 in populations with health disparities: Posited involvement of mitochondrial disorder, socioeconomic stress, and pollutants. Journal of Biochemical and Molecular Toxicology. 2021; 35: e22626.

[17] Xu W, Zhao T, Xiao H. The Implication of Oxidative Stress and AMPK-Nrf2 Antioxidative Signaling in Pneumonia Pathogenesis. Frontiers in Endocrinology. 2020; 11: 400.

[18] Jakubczyk K, Dec K, Kałduńska J, Kawczuga D, Kochman J, Janda K. Reactive oxygen species - sources, functions, oxidative damage. Polski Merkuriusz Lekarski: Organ Polskiego Towarzystwa Lekarskiego. 2020; 48: 124–127.

[19] Wu J. Tackle the free radicals damage in COVID-19. Nitric Oxide: Biology and Chemistry. 2020; 102: 39–41.

[20] Iddir M, Brito A, Dingeo G, Fernandez Del Campo SS, Samouda H, La Frano MR, *et al*. Strengthening the Immune System and Reducing Inflammation and Oxidative Stress through Diet and Nutrition: Considerations during the COVID-19 Crisis. Nutrients. 2020; 12: 1562.

[21] McAllister MJ, Kirkwood K, Chuah SC, Thompson EJ, Cartwright JA, Russell CD, *et al*. Intestinal Protein Characterisation of SARS-CoV-2 Entry Molecules ACE2 and TMPRSS2 in Inflammatory Bowel Disease (IBD) and Fatal COVID-19 Infection. Inflammation. 2022; 45: 567–572.

[22] Liu ZH, Zhang Y, Wang X, Fan XF, Zhang Y, Li X, *et al*. SIRT1 activation attenuates cardiac fibrosis by endothelial-to-mesenchymal transition. Biomedicine & Pharmacotherapy. 2019; 118: 109227.

[23] Hwang HJ, Kim N, Herman AB, Gorospe M, Lee JS. Factors and Pathways Modulating Endothelial Cell Senescence in Vascular Aging. International Journal of Molecular Sciences. 2022; 23: 10135.

[24] Xu J, Núñez G. The NLRP3 inflammasome: activation and regulation. Trends in Biochemical Sciences. 2023; 48: 331–344.

[25] Napodano C, Carnazzo V, Basile V, Pocino K, Stefanile A, Gallucci S, *et al*. NLRP3 Inflammasome Involvement in Heart, Liver, and Lung Diseases-A Lesson from Cytokine Storm Syndrome. International Journal of Molecular Sciences. 2023; 24: 16556.

[26] Stotts C, Corrales-Medina VF, Rayner KJ. Pneumonia-Induced Inflammation, Resolution and Cardiovascular Disease: Causes, Consequences and Clinical Opportunities. Circulation Research. 2023; 132: 751–774.

[27] Feng Y, Li M, Yangzhong X, Zhang X, Zu A, Hou Y, *et al*. Pyroptosis in inflammation-related respiratory disease. Journal of Physiology and Biochemistry. 2022; 78: 721–737.